Electronic structure calculations with interpolating tensor product wavelet basis

Tommi Höynälänmaa [*] and Tapio T. Rantala [†]
Computational Physics, P. O. Box 692, FI-33014 Tampere University, Finland

(Received 21 March 2023; accepted 4 August 2023; published 22 August 2023)

We introduce a basis set consisting of three-dimensional Deslauriers-Dubuc wavelets and solve numerically the Schrödinger equations of H and He atoms and molecules H_2, H_2^+, and LiH with Hartree-Fock and density functional theory (DFT) methods. We also compute the $2s$ and $2p$ excited states of hydrogen. The Coulomb singularity at the nucleus is handled by using a pseudopotential. The eigenvalue problem is solved with Arnoldi and Lanczos methods, Poisson equation with generalized minimal residual method and conjugate gradient on the normal equations methods, and matrix elements are computed using the biorthogonality relations of the interpolating wavelets. Performance is compared with those of CCCBDB and BIGDFT.

DOI: 10.1103/PhysRevE.108.025307

I. INTRODUCTION

Standard approaches to assess properties of atoms, molecules and models of nanostructures in quantum chemistry are Hartree-Fock (HF) and density functional theory (DFT). Both of these invoke numerical solutions of the Schrödinger differential equation of the many-body system of electrons. Thus, controlled approximations are inevitable and practical numerical algorithms are necessary.

The vast majority of the algorithms are based on finding the solutions or orbitals as series expansion of basis functions, the basis set. A finite basis set leads to the Roothaan-Hall equations, a generalized matrix eigenvalue problem. Gaussian-type basis functions are the most popular due to their advantageous analytical features. Here, we introduce a different type basis set, wavelet functions, point out their advantages and drawbacks, and consider a few test cases and compare their performance with conventional approaches.

Wavelets and related scaling functions are functions generated by translations and dilatations of the so-called mother wavelet and mother scaling function. Interpolating wavelets use a mother scaling function satisfying the cardinal interpolating property $\varphi(k) = \delta_{k,0}$ where k is an integer. Orthonormal wavelets form an orthonormal basis in function space $L^2(\mathbb{R})$. Both of these wavelet types can be generalized to multivariate functions.

Studies of wavelets have been active, and new ones with various properties have been found during the past tens of years [1,2]. One-dimensional interpolating wavelets in function space $C_u(\mathbb{R})$ consisting of bounded and uniformly continuous functions on $\mathbb{R}$ are defined in Ref. [2]. One-dimensional interpolating wavelets in function space $C_0(\mathbb{R})$ consisting of functions on $\mathbb{R}$ vanishing at infinity are defined in Ref. [3]. Deslauriers-Dubuc wavelets have also been discussed in Refs. [4,5]. Compactly supported interpolating wavelets have been generalized to multiple dimensions in Refs. [6,7]. Fukuda, Kinoshita, and Suzuki [8] have studied unconditional convergence of wavelet expansions. They have shown that uniformly convergent wavelet expansions even for continuous functions do not always converge unconditionally in $L^\infty(\mathbb{R})$. Pathak [9] has investigated translation and convolution associated with discrete wavelet transform.

Arias [10] and Engeness and Arias [11] have developed formalism for electronic structure calculations with interpolating wavelets so that matrix elements of the operators are computed as usual and overlap matrices are used in the matrix form of the Schrödinger equation. Lippert *et al.* [12] introduce a Lagrangian based formalism for the multiresolution analysis (MRA) of electronic structure. Arias [10] uses a carbon atom and a N_2 molecule as examples. Engeness and Arias [11] use both calcium and aluminum atoms and molecules O_2 and H_2O as examples.

Fischer and Defranceschi use Daubechies wavelets [1] for computation of hydrogenlike atoms [13]. They have developed an iterative method based on nonstandard operator form of the Schrödinger operator. Their work shows that this method is well suited for computations of hydrogenlike atoms. Fischer and Defranceschi have presented Hartree-Fock equations in an orthonormal wavelet basis [14]. They have also analyzed the Hartree-Fock method with a continuous wavelet transform [15] and demonstrated it using the hydrogenic Schrödinger equation with an iterative solution scheme.

Wei and Chou [16] have used orthonormal wavelets in self-consistent electronic structure calculations within the local-density approximation and demonstrated their method with H_2 and O_2 molecules. Tymczak and Wang [17] have used orthonormal Daubechies wavelets for quantum molecular dynamic simulations and developed a wavelet selection scheme for computations. They used a hydrogen atom and a H_2 molecule as examples. Their method shows systematic convergence with increasing grid size. Yamaguchi and Mukoyama [18] have carried out electronic structure calculations with the Hartree-Fock method and Meyer wavelets.

[*]Corresponding author: tommi.hoynalanmaa@tuni.fi
[†]tapio.rantala@tuni.fi

Our earlier contribution [19] is use of one-dimensional interpolating wavelets to solve the Hartree-Fock equations in the central field approximation for orbitals of several test case atoms. We were able to derive analytic formulas for all the relevant matrix elements of Hamiltonian and Fock operators. We also developed the exact pseudopotential method [20] for one-dimensional calculations of atoms and applied it to the hydrogen and helium ground states and for some excited states.

Iyengar and Frisch [21] have studied relationship between Gaussian basis sets and wavelets. They use a time-dependent basis function set: Gaussian functions centered at nuclei of the system. When the nuclei move the basis functions move, too. Gaussian functions are an example of *multiwavelets* [21–23] for which the Jth level scaling space is decomposed into N-scaling spaces via

$$\cdots \mathbf{V}_{J-1}^{(N)} \subset \mathbf{V}_J^{(1)} \subset \mathbf{V}_J^{(2)} \subset \cdots \subset \mathbf{V}_J^{(N)} \subset \mathbf{V}_{J+1}^{(1)} \cdots . \quad (1)$$

Comparative studies of wavelets and Gaussian functions are presented, e.g., in Refs. [24,25]. Harrison *et al.* [26] use multiwavelets for quantum chemistry computations. Yanai *et al.* [27] present a numerical algorithm to evaluate Hartree-Fock exchange in the self-consistent field method. Yanai *et al.* [28,29] develop a method to do time-dependent Hartree-Fock and density functional theory computation with multiwavelets. Jensen *et al.* [30] perform multiwavelet computations of total energies with generalized gradient approximation-Perdew-Burke-Ernzerhof (PBE) and hybrid-PBE0 density functionals for 211 molecules. Jensen *et al.* [31] compute some magnetic properties with multiwavelets.

Han *et al.* [32] have developed an all-electron density-functional program using the Mexican hat wavelets. They analyze H_2, CO, and H_2O molecules and 1s core-ionized C*O and CO* molecules. Their method shows very good performance over the plane-wave-based methods. Genovese *et al.* [33] and Mohr *et al.* [34] have composed a software package BIGDFT that implements the DFT method for quantum physical systems using three-dimensional Daubechies wavelets as a basis function set.

In three-dimensional space, the number of basis functions may grow relatively large to give sufficient accuracy. Therefore, we do not construct the Hamiltonian matrix explicitly. Instead, we use iterative algorithms in solving the Roothaan-Hall equation, though correspondingly, the computation gets slower in self-consistent iteration of Hartree-Fock or DFT orbitals for many electron systems.

In this paper, we demonstrate evaluation of electronic structure with three-dimensional interpolating tensor product wavelets and use of dual multiresolution analysis in computation of the matrix elements of the various operators. We make calculations for the hydrogen and helium atoms, the hydrogen molecule ion, the hydrogen molecule, and the lithium hydride molecule. Self-consistent iteration, Hartree-Fock, and DFT methods are used for many electron systems. Pseudopotentials are used for two different purposes to handle the Coulomb singularity at nuclei and also as the frozen core. We use the data from BIGDFT as the reference for our calculations with the interpolating tensor product Deslauriers-Dubuc wavelet basis function set.

An advantage of the interpolating wavelets compared to the orthonormal wavelets is that computing a wavelet expansion of the function does not require numerical evaluation of integrals since the dual wavelets are weighted sums of δ functions. In case the interpolating wavelets are compactly supported, these sums are finite, too. We have to choose the wavelet family so that its Hölder regularity is, at least, 2 in order to enable the evaluation of the Laplacian operator. BIGDFT uses Daubechies orthonormal wavelets for the computation of atomic orbitals and scalar products and interpolating wavelets for charge density, function products, and the Poisson solver. We use a rectangular computation grid, whereas, BIGDFT uses a spherical one.

From now on, we use atomic units throughout this article ($e = m_e = \hbar = 4\pi\varepsilon_0 = 1$). Thus, units for energy and length, "Hartree" and "Bohr" are used and abbreviated as (Ha) and (B). Notations for wavelet basis functions and filters is similar to that in Ref. [6] and computation of matrix elements is similar to that in Ref. [7].

II. SOLVING THE SCHRÖDINGER EQUATIONS

A. General

Consider a system with n electrons and m nuclei with atomic numbers Z_i and locations $\mathbf{R}_i$. Within the Born-Oppenheimer approximation, dynamics of electrons and nuclei are independent, and then, the wave function separates to two factors, correspondingly. Here, we consider the electronic part, the orbitals, only, and keep the nuclear conformation $\{\mathbf{R}_i\}$ fixed.

With the fixed nuclear conformation, the Coulomb potential for dynamics of electrons is

$$V_{\mathrm{N}}(\mathbf{r}) = -\sum_{i=1}^{m} \frac{Z_i}{|\mathbf{r} - \mathbf{R}_i|}, \quad (2)$$

and the internuclear repulsion energy,

$$E_{\mathrm{R}} = \sum_{i=1}^{m-1} \sum_{j>i}^{m} \frac{Z_i Z_j}{|\mathbf{R}_i - \mathbf{R}_j|}. \quad (3)$$

For an atom, we have $E_{\mathrm{R}} = 0$.

Let us denote the orbitals by ϕ as symbols φ and ψ are used for scaling functions and wavelets.

If the spacing between grid points is a (usually negative) power of 2, we can handle this by choosing $j_{\min}$ in Eqs. (25) and (26) properly. Otherwise, we have to make a change in variables $\mathbf{r} = a\mathbf{r}'$ in the Schrödinger equation. Here, one unit in the computation grid corresponds to a Bohrs.

B. Single-electron system

The Schrödinger equation of a single-electron system is

$$\left(-\tfrac{1}{2}\nabla^2 + V_{\mathrm{N}}\right)\phi = \varepsilon\phi, \quad (4)$$

where ε is the orbital energy and the total energy including nuclear repulsion is

$$E_{\mathrm{total}} = \varepsilon + E_{\mathrm{R}}. \quad (5)$$

The wave equation of a single-electron system is solved by the implicitly restarted Arnoldi method [35,36]. The Arnoldi method is able to find also other than the lowest eigenvalue.

C. Hartree-Fock method

The HF equation for an n electron system is

$$\left(-\tfrac{1}{2}\nabla^2 + V_{\rm N} + V_{\rm H} + V_{\rm x}^i\right)\phi_i = \varepsilon_i\phi_i, \tag{6}$$

where the Hartree potential is given by

$$V_{\rm H}(\mathbf{r}) = \int_{\mathbb{R}^3} \rho(\mathbf{r}')\frac{1}{|\mathbf{r}-\mathbf{r}'|}d^3\mathbf{r}', \tag{7}$$

and the charge density by

$$\rho(\mathbf{r}) = \sum_{i=1}^{n} |\phi_i(\mathbf{r})|^2. \tag{8}$$

The exchange potentials V_x^i, $i = 1, \ldots, n$, are defined in Ref. [37], Sec. 2.2 but not needed in our paper. For a two-electron system with both electrons occupying the same orbital as the singlet state HF equation can be written as

$$\left(-\tfrac{1}{2}\nabla^2 + V_{\rm N} + \tfrac{1}{2}V_{\rm H}\right)\phi_1 = \varepsilon_1\phi_1. \tag{9}$$

The Hartree potential is computed by solving the Poisson equation,

$$\nabla^2 V_{\rm H} = -4\pi\rho, \tag{10}$$

numerically.

In this case where there are more than one resolution level in an interpolating wavelet basis, the matrix L of the Laplacian operator is not generally Hermitian, so we cannot solve Eq. (10) directly with the conjugate gradient method. The non-Hermiticity arises because our matrix elements are not computed as ordinary inner products between functions. In this case, we use one of the following two methods:

(1) conjugate gradient on the normal equations (CGNR): solve

$$L^T L V_{\rm H} = -4\pi L^T\rho, \tag{11}$$

with the conjugate gradient method.

(2) Generalized minimal residual method (GMRES) [38].

When the basis set consists of a single resolution level, we may the use ordinary conjugate gradient method to solve (10).

The total energy of a two electron system is

$$E_{\rm total} = 2\varepsilon_1 - \frac{1}{4}\int_{\mathbb{R}^3}\rho(\mathbf{r})V_{\rm H}(\mathbf{r})d^3\mathbf{r} + E_{\rm R}. \tag{12}$$

In this paper, we consider restricted Hartree-Fock approach, only.

D. Density functional theory and local density approximation

Suppose that we have a system with M electronic orbitals whose total wave functions are Ψ. The Kohn-Sham equation [37,39,40] for the electronic structure is

$$\left(-\tfrac{1}{2}\nabla^2 + V_{\rm N} + V_{\rm H} + V_{\rm xc}[\rho]\right)\phi_i = E_i\phi_i, \tag{13}$$

where the charge density is

$$\rho(\mathbf{r}_1) = \sum_{s_1=\pm 1/2} M\int |\Psi(\mathbf{x}_1, \mathbf{x}_2, \ldots, \mathbf{x}_M)|^2 d\mathbf{x}_2\cdots d\mathbf{x}_M, \tag{14}$$

and the Hartree potential,

$$V_{\rm H}(\mathbf{r}) = \int_{\mathbb{R}^3}\rho(\mathbf{r}')\frac{1}{|\mathbf{r}-\mathbf{r}'|}d^3\mathbf{r}', \tag{15}$$

and $V_{\rm xc}[\rho]$ is the *exchange-correlation potential*. We have

$$V_{\rm xc}[\rho] = V_{\rm x}[\rho] + V_{\rm c}[\rho], \tag{16}$$

where $V_{\rm x}[\rho]$ is the *exchange potential* and $V_{\rm c}[\rho]$ is the *correlation potential*. In this article, we set $V_{\rm c}[\rho] = 0$. The exchange-correlation energy is defined by

$$E_{\rm xc}[\rho] = E_{\rm x}[\rho] + E_{\rm c}[\rho], \tag{17}$$

where $E_{\rm x}[\rho]$ is the *exchange energy* and $E_{\rm c}[\rho]$ is the *correlation energy*. In this article, we ignore the correlation energy.

Within the local density approximation (LDA), we define

$$E_{\rm x}[\rho] = \int \rho(\mathbf{r})\varepsilon_{\rm x}[\rho](\mathbf{r})d^3\mathbf{r}, \tag{18}$$

where $\varepsilon_{\rm x}[\rho](\mathbf{r})$ is the exchange energy per particle of a uniform electron gas at a density of ρ. It follows from the Kohn-Sham theorem [37], Sec. 3.1 that the exchange potential is

$$V_{\rm x}[\rho] = \frac{\delta E_{\rm x}[\rho]}{\delta\rho}. \tag{19}$$

We have

$$E_{\rm x}[\rho] = -\frac{3}{4}\left(\frac{3}{\pi}\right)^{1/3}\int[\rho(\mathbf{r})]^{4/3}d^3\mathbf{r}, \tag{20}$$

and

$$V_{\rm x}[\rho](\mathbf{r}) = -\left(\frac{3}{\pi}\rho(\mathbf{r})\right)^{1/3}. \tag{21}$$

The total energy of the system is

$$E_{\rm KS} = \sum_{i=1}^{n} E_i - \frac{1}{2}\int\rho(\mathbf{r})V_{\rm H}(\mathbf{r})d^3\mathbf{r} + E_{\rm xc}[\rho] - \int\rho(\mathbf{r})V_{\rm xc}[\rho](\mathbf{r})d^3\mathbf{r}. \tag{22}$$

The Kohn-Sham equations are solved by a similar self-consistent iteration as the HF equations.

III. THREE-DIMENSIONAL WAVELET BASIS SET

A. The basis set

Let $j_{\rm min}$ and $j_{\rm max}$ be the minimum and maximum resolution levels of the point grid. Let

$$Z_j = \left\{\frac{k}{2^j}\middle| k\in\mathbb{Z}\right\}, \tag{23}$$

and

$$V_j = Z_j^3, \tag{24}$$

where $j \in \mathbb{Z}$. Define sets Q_j by

$$Q_{j_{\min}} = V_{j_{\min}}, \tag{25}$$

$$Q_j = V_j \setminus V_{j-1} \quad \text{for } j > j_{\min}. \tag{26}$$

The point grid G will be some finite subset of $V_{j_{\max}}$. We define

$$G_j := G \cap Q_j \tag{27}$$

for $j \geqslant j_{\min}$. The functions $\varphi_{j,k}$ and $\psi_{j,k}$ are scaling functions and wavelets belonging to an interpolating wavelet family. Functions $\tilde{\varphi}_{j,k}$ and $\tilde{\psi}_{j,k}$ are dual basis functions of interpolating wavelets.

Define

$$\psi_{s,j,k} := \begin{cases} \varphi_{j,k}, & \text{if } s = 0, \\ \psi_{j,k}, & \text{if } s = 1, \end{cases} \tag{28}$$

$$\tilde{\psi}_{s,j,k} := \begin{cases} \tilde{\varphi}_{j,k}; & \text{if } s = 0, \\ \tilde{\psi}_{j,k}; & \text{if } s = 1, \end{cases} \tag{29}$$

and

$$\eta_{j,k} := \begin{cases} \varphi_{j_{\min},k}, & \text{if } j = j_{\min}, \\ \varphi_{j-1,k/2}, & \text{if } j > j_{\min} \text{ and } k \text{ even}, \\ \psi_{j-1,(k-1)/2}, & \text{if } j > j_{\min} \text{ and } k \text{ odd}, \end{cases} \tag{30}$$

$$\tilde{\eta}_{j,k} := \begin{cases} \tilde{\varphi}_{j_{\min},k}, & \text{if } j = j_{\min}, \\ \tilde{\varphi}_{j-1,k/2}, & \text{if } j > j_{\min} \text{ and } k \text{ even}, \\ \tilde{\psi}_{j-1,(k-1)/2}, & \text{if } j > j_{\min} \text{ and } k \text{ odd}. \end{cases} \tag{31}$$

When $\alpha \in Q_j$ and $j \geqslant j_{\min}$ define

$$\zeta_\alpha := \eta_{j,\mathbf{k}[1]} \otimes \eta_{j,\mathbf{k}[2]} \otimes \eta_{j,\mathbf{k}[3]}, \tag{32}$$

and

$$\tilde{\zeta}_\alpha := \tilde{\eta}_{j,\mathbf{k}[1]} \otimes \tilde{\eta}_{j,\mathbf{k}[2]} \otimes \tilde{\eta}_{j,\mathbf{k}[3]}, \tag{33}$$

where $\mathbf{k} = 2^j \alpha$. We also define

$$\varphi_{j,\mathbf{k}} := \varphi_{j,\mathbf{k}[1]} \otimes \varphi_{j,\mathbf{k}[2]} \otimes \varphi_{j,\mathbf{k}[3]}, \tag{34}$$

where $j \in \mathbb{Z}$ and $\mathbf{k} \in \mathbb{Z}^3$.

B. Backward and forward wavelet transforms

Let

$$f = \sum_{\alpha \in G} c_\alpha \zeta_\alpha, \tag{35}$$

where $c_\alpha \in \mathbb{R}$ for all $\alpha \in G$'s. Let $c = (c_\alpha)_{\alpha \in G}$. Define $v = (v_\alpha)_{\alpha \in G}$ by setting

$$v_\alpha = f(\alpha). \tag{36}$$

We define forward wavelet transform U and backward wavelet transform W by setting $U(v) = c$ and $W(c) = v$. Mappings U and W are linear. We compute the forward wavelet transform U using an algorithm somewhat similar to Ref. [41]. Define matrix $P^{(j)}$ by

$$P^{(j)}_{\alpha,\beta} = \delta_{\alpha,\beta}, \tag{37}$$

where $\alpha \in G_j$, $\beta \in G$, and matrix $E^{(j)}$ by

$$E^{(j)}_{\alpha,\beta} = \delta_{\alpha,\beta}, \tag{38}$$

where $\alpha \in G$ and $\beta \in G_j$. Define

$$W^{(j,j')}_{\alpha,\beta} = \zeta_\beta(\alpha), \tag{39}$$

where $\alpha \in G_j$ and $\beta \in G_{j'}$. See Eq. (27) for definition of G_j and Eq. (32) for the definition of ζ_β. We have

$$W = \sum_{j=j_{\min}}^{j_{\max}} \sum_{j'=j_{\min}}^{j} E^{(j)} W^{(j,j')} P^{(j')}. \tag{40}$$

For forward wavelet transform, we have

$$U = \sum_{j=j_{\min}}^{j_{\max}} E^{(j)} U^{(j)}, \tag{41}$$

$$U^{(j)} = J^{(j)} \left(P^{(j)} - \sum_{j'=j_{\min}}^{j-1} W^{(j,j')} U^{(j')} \right) \quad \text{for } j > j_{\min}, \tag{42}$$

$$U^{(j_{\min})} = P^{(j_{\min})}, \tag{43}$$

$$J^{(j)} = (W^{(j,j)})^{-1}. \tag{44}$$

When

$$f = \sum_{\beta \in G_j} c_\beta \zeta_\beta, \tag{45}$$

we have

$$c_\alpha = \langle \tilde{\zeta}_\alpha, f \rangle = \left\langle \tilde{\zeta}_\alpha, \sum_{\beta \in G_j} f(\beta) \varphi_{j,2^j\beta} \right\rangle = \sum_{\beta \in G_j} \langle \tilde{\zeta}_\alpha, \varphi_{j,2^j\beta} \rangle f(\beta). \tag{46}$$

Consequently,

$$J^{(j)}_{\alpha,\beta} = \langle \tilde{\zeta}_\alpha, \varphi_{j,2^j\beta} \rangle, \tag{47}$$

and we do not have to invert matrix $W^{(j,j)}$.

An operator representing pointwise multiplication of a function f by another in the given computation grid is

$$M = UDW, \tag{48}$$

where D is a diagonal matrix with values of the function f at the grid points in the diagonal. The local pseudopotentials are computed this way.

C. Matrix elements of the Laplacian operator

Laplacian operator,

$$\nabla^2 = \frac{\partial^2}{\partial x^2} + \frac{\partial^2}{\partial y^2} + \frac{\partial^2}{\partial z^2} \tag{49}$$

is approximated by linear operator $L = L^{(x)} + L^{(y)} + L^{(z)}$ where

$$L^{(x)}_{\alpha,\alpha'} = \int_{\mathbb{R}^3} \tilde{\zeta}_\alpha(\mathbf{x}) \frac{\partial^2}{\partial x^2} \zeta_{\alpha'}(\mathbf{x}) d\tau, \tag{50}$$

$$L^{(y)}_{\alpha,\alpha'} = \int_{\mathbb{R}^3} \tilde{\zeta}_\alpha(\mathbf{x}) \frac{\partial^2}{\partial y^2} \zeta_{\alpha'}(\mathbf{x}) d\tau, \tag{51}$$

$$L^{(z)}_{\alpha,\alpha'} = \int_{\mathbb{R}^3} \tilde{\zeta}_\alpha(\mathbf{x}) \frac{\partial^2}{\partial z^2} \zeta_{\alpha'}(\mathbf{x}) d\tau \tag{52}$$

for $\alpha, \alpha' \in G$. Let $\alpha = 2^{-j}(k_x, k_y, k_z) \in G \cap Q_j$ and $\alpha' = 2^{-j'}(k'_x, k'_y, k'_z) \in G \cap Q_{j'}$. We define

$$\iota = \begin{cases} j-1, & \text{if } j > j_{\min}, \\ j, & \text{if } j = j_{\min}, \end{cases} \tag{53}$$

$$l_x = \begin{cases} \frac{k_x}{2}, & \text{if } k_x \text{even and } j > j_{\min}, \\ \frac{k_x-1}{2}, & \text{if } k_x \text{ odd and } j > j_{\min}, \\ k_x, & \text{if } j = j_{\min}, \end{cases} \tag{54}$$

$$t_x = \begin{cases} 0, & \text{if } j = j_{\min} \text{ or } j > j_{\min} \text{ and } k_x \text{ even}, \\ 1, & \text{if } j > j_{\min} \text{ and } k_x \text{ odd}, \end{cases} \tag{55}$$

$$l_y = \begin{cases} \frac{k_y}{2}, & \text{if } k_y \text{ even and } j > j_{\min}, \\ \frac{k_y-1}{2}, & \text{if } k_y \text{ odd and } j > j_{\min}, \\ k_y, & \text{if } j = j_{\min}, \end{cases} \tag{56}$$

$$t_y = \begin{cases} 0, & \text{if } j = j_{\min} \text{ or } j > j_{\min}, \text{ and } k_y \text{ even}, \\ 1, & \text{if } j > j_{\min}, \text{ and } k_y \text{ odd}, \end{cases} \tag{57}$$

$$l_z = \begin{cases} \frac{k_z}{2}, & \text{if } k_z \text{ even and } j > j_{\min}, \\ \frac{k_z-1}{2}, & \text{if } k_z \text{ odd and } j > j_{\min}, \\ k_z, & \text{if } j = j_{\min}, \end{cases} \tag{58}$$

$$t_z = \begin{cases} 0, & \text{if } j = j_{\min} \text{ or } j > j_{\min}, \text{ and } k_z \text{ even}, \\ 1, & \text{if } j > j_{\min} \text{ and } k_z \text{ odd}, \end{cases} \tag{59}$$

and similar definitions for $\iota', l'_x, t'_x, l'_y, t'_y, l'_z$, and t'_z. Elements of matrices are computed by

$$L^{(x)}_{\alpha,\alpha'} = \begin{cases} 2^{2\iota} a(t_x, t'_x, \iota' - \iota, l'_x - 2^{\iota'-\iota} l_x) \\ \times s(t_y, t'_y, \iota' - \iota, l'_y - 2^{\iota'-\iota} l_y) \\ \times s(t_z, t'_z, \iota' - \iota, l'_z - 2^{\iota'-\iota} l_z), & \text{if } \iota \leqslant \iota', \\ 2^{2\iota'} a(t_x, t'_x, \iota' - \iota, l_x - 2^{\iota-\iota'} l'_x) \\ \times s(t_y, t'_y, \iota' - \iota, l_y - 2^{\iota-\iota'} l'_y) \\ \times s(t_z, t'_z, \iota' - \iota, l_z - 2^{\iota-\iota'} l'_z), & \text{if } \iota > \iota', \end{cases} \tag{60}$$

$$L^{(y)}_{\alpha,\alpha'} = \begin{cases} 2^{2\iota} s(t_x, t'_x, \iota' - \iota, l'_x - 2^{\iota'-\iota} l_x) \\ \times a(t_y, t'_y, \iota' - \iota, l'_y - 2^{\iota'-\iota} l_y) \\ \times s(t_z, t'_z, \iota' - \iota, l'_z - 2^{\iota'-\iota} l_z), & \text{if } \iota \leqslant \iota', \\ 2^{2\iota'} s(t_x, t'_x, \iota' - \iota, l_x - 2^{\iota-\iota'} l'_x) \\ \times a(t_y, t'_y, \iota' - \iota, l_y - 2^{\iota-\iota'} l'_y) \\ \times s(t_z, t'_z, \iota' - \iota, l_z - 2^{\iota-\iota'} l'_z), & \text{if } \iota > \iota', \end{cases} \tag{61}$$

$$L^{(z)}_{\alpha,\alpha'} = \begin{cases} 2^{2\iota} s(t_x, t'_x, \iota' - \iota, l'_x - 2^{\iota'-\iota} l_x) \\ \times s(t_y, t'_y, \iota' - \iota, l'_y - 2^{\iota'-\iota} l_y) \\ \times a(t_z, t'_z, \iota' - \iota, l'_z - 2^{\iota'-\iota} l_z), & \text{if } \iota \leqslant \iota', \\ 2^{2\iota'} s(t_x, t'_x, \iota' - \iota, l_x - 2^{\iota-\iota'} l'_x) \\ \times s(t_y, t'_y, \iota' - \iota, l_y - 2^{\iota-\iota'} l'_y) \\ \times a(t_z, t'_z, \iota' - \iota, l_z - 2^{\iota-\iota'} l'_z), & \text{if } \iota > \iota'. \end{cases} \tag{62}$$

The filters a and s are defined by

$$a(t_1, t_2, j, k) = \int_{\mathbb{R}^3} \tilde{\psi}_{t_1,0,0}(x) \frac{\partial^2}{\partial x^2} \psi_{t_2,j,k}(x) d\tau, \quad \text{for } j \geqslant 0, \tag{63}$$

$$a(t_1, t_2, j, k) = \int_{\mathbb{R}^3} \tilde{\psi}_{t_1,-j,k}(x) \frac{\partial^2}{\partial x^2} \psi_{t_2,0,0}(x) d\tau, \quad \text{for } j < 0, \tag{64}$$

$$s(t_1, t_2, j, k) = \int_{\mathbb{R}^3} \tilde{\psi}_{t_1,0,0}(x) \psi_{t_2,j,k}(x) d\tau, \quad \text{for } j \geqslant 0, \tag{65}$$

$$s(t_1, t_2, j, k) = \int_{\mathbb{R}^3} \tilde{\psi}_{t_1,-j,k}(x) \psi_{t_2,0,0}(x) d\tau, \quad \text{for } j < 0. \tag{66}$$

Filter a is computed with formulas

$$a(0, 0, j, k) = 2^{2j} a_0(k) \quad \text{for } j \geqslant 0, \tag{67}$$

$$a(0, 0, -1, k) = 4 \sum_{\mu=-m}^{m} h_\mu a(0, 0, 0, \mu - k) \quad \text{for } j = -1, \tag{68}$$

$$a(0, 0, j, k) = 4 \sum_{\mu=-m}^{m} h_\mu a(0, 0, j+1, k - 2^{-j-1}\mu) \quad \text{for } j < -1, \tag{69}$$

$$a(0, 1, j, k) = a(0, 0, j+1, 2k+1) \quad \text{for } j \geqslant 0, \tag{70}$$

$$a(0, 1, -1, k) = 4a_0(1-k), \tag{71}$$

$$a(0, 1, j, k) = 4a(0, 0, j+1, k - 2^{-j-1}) \quad \text{for } j < -1, \tag{72}$$

$$a(1, 0, 0, k) = \sum_{\nu=-m}^{m} \tilde{g}_\nu a(0, 0, -1, \nu - 2k), \tag{73}$$

$$a(1, 0, j, k) = 4 \sum_{\nu=-m}^{m} \tilde{g}_\nu a(0, 0, j-1, k - 2^{j-1}\nu) \quad \text{for } j > 0, \tag{74}$$

$$a(1, 0, j, k) = \sum_{\nu=-m}^{m} \tilde{g}_\nu a(0, 0, j-1, 2k+\nu) \quad \text{for } j < 0, \tag{75}$$

$$a(1, 1, j, k) = a(1, 0, j+1, 2k+1) \quad \text{for } j \geqslant 0, \tag{76}$$

$$a(1, 1, -1, k) = 4a(1, 0, 0, 1-k), \tag{77}$$

$$a(1, 1, j, k) = 4a(1, 0, j+1, k - 2^{-j-1}) \quad \text{for } j < -1, \tag{78}$$

where

$$a_0(k) := \int_{\mathbb{R}} \tilde{\varphi}(x) \frac{\partial^2}{\partial x^2} \varphi(x - k) dx. \tag{79}$$

Filter s is computed with formulas,

$$s(0, 0, j, k) = \delta_{k,0} \quad \text{for } j \geqslant 0, \tag{80}$$

$$s(0, 0, -1, k) = h_k, \tag{81}$$

$$s(0,0,j,k) = \sum_{\mu=-m}^{m} h_\mu s(0,0,j+1,k-2^{-j-1}\mu)$$

$$\text{for } j < -1, \tag{82}$$

$$s(0,1,j,k) = 0 \quad \text{for } j \geqslant 0, \tag{83}$$

$$s(0,1,-1,k) = \delta_{k,1}, \tag{84}$$

$$s(0,1,j,k) = s(0,0,j+1,k-2^{-j-1}) \quad \text{for } j < -1, \tag{85}$$

$$s(1,0,0,k) = 0, \tag{86}$$

$$s(1,0,j,k) = \sum_{\nu=-m}^{m} \tilde{g}_\nu \delta_{k,2^{j-1}\nu} \quad \text{for } j > 0, \tag{87}$$

$$s(1,0,j,k) = 0 \quad \text{for } j < 0, \tag{88}$$

$$s(1,1,0,k) = \delta_{k,0}, \tag{89}$$

$$s(1,1,j,k) = 0 \quad \text{for } j \neq 0. \tag{90}$$

IV. CONSTANT AND INTERPOLATED PSEUDOPOTENTIALS

The Coulomb potential arising from a single nucleus is

$$V(r) = -\frac{Z}{r}, \tag{91}$$

where Z is the charge of the nucleus.

We avoid the singularity by using a pseudopotential. We define c to be the cutoff point of the pseudopotential, and D to be the degree of the interpolating polynomial used in the pseudopotential. Actually, we use $c = 2^{-j_{\max}}$ where $j_{\max}$ is the highest resolution level in the wavelet basis. Parameter D has to be an odd integer, and we define $n = (D+1)/2$. We define

$$V_1(r) := -\frac{1}{r}, \quad r \geqslant 0, \tag{92}$$

$$\mathbf{s} := [-nc, \ -(n-1)c, \ldots, -2c, -c, c, 2c, \ldots, (n-1)c, nc], \tag{93}$$

and

$$\mathbf{t}[i] := V_1(\mathbf{s}[i]), \tag{94}$$

where $i = 1, \ldots, 2n$. Let P be the interpolating polynomial of degree at most D having value $\mathbf{t}[i]$ at point $\mathbf{s}[i]$ for $i = 1, \ldots, 2n$. Now, we define the interpolated pseudopotential with

$$V_{\text{interp}}(r) := \begin{cases} V_1(r), & r \geqslant c, \\ P(r), & r < c. \end{cases} \tag{95}$$

The actual pseudopotential of a nucleus with charge Z and location $\mathbf{R}$ is then

$$V(\mathbf{r}) = ZV_{\text{interp}}(|\mathbf{r} - \mathbf{R}|). \tag{96}$$

Function V_{interp} with different values of c is plotted in Fig. 1. We may also use the cut pseudopotential defined by

$$V_{\text{cut}}(r) := \begin{cases} V_1(r), & r \geqslant c, \\ -\frac{1}{c}, & r < c, \end{cases} \tag{97}$$

where $c = 2^{-j_{\max}-1}$.

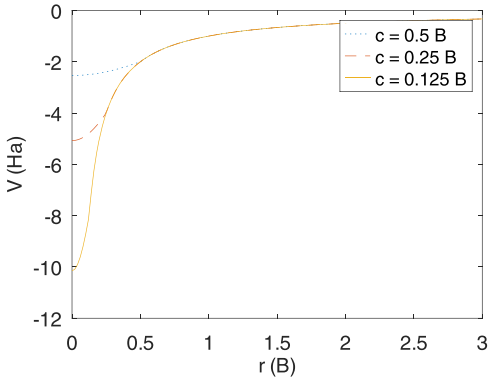

FIG. 1. Pseudopotentials V_{interp} with $D = 7$. Parameter c is the cutoff value, see Sec. IV.

V. HARTWIGSEN-GOEDECKER-HUTTER PSEUDOPOTENTIAL

By using pseudopotentials the number of computed orbitals can be reduced and since the pseudo wave functions are smoother than all-electron wave functions the basis function set can also be reduced. In a pseudopotential computation only, the valence electrons are actually computed, and the effect of the core electrons is handled by replacing the nuclear potential with a pseudopotential. We use the Hartwigsen-Goedecker-Hutter (HGH) pseudopotential [33,42] in these computations.

The HGH pseudopotential consists of a local and a nonlocal part. The local part is a function of the position as the nuclear potential. The nonlocal part is a linear operator, and it is not a function of position. The local pseudopotential is given by

$$V_{\text{loc}}(r) = \frac{-Z_{\text{ion}}}{r}\text{erf}\left(\frac{r}{\sqrt{2}r_{\text{loc}}}\right) + \exp\left[-\frac{1}{2}\left(\frac{r}{r_{\text{loc}}}\right)^2\right] \times \left[C_1 + C_2\left(\frac{r}{r_{\text{loc}}}\right)^2 + C_3\left(\frac{r}{r_{\text{loc}}}\right)^4 + C_4\left(\frac{r}{r_{\text{loc}}}\right)^6\right]$$

where r is the distance from the nucleus. Note that

$$\lim_{r\to 0} \frac{-Z_{\text{ion}}}{r}\text{erf}\left(\frac{r}{\sqrt{2}r_{\text{loc}}}\right) = \frac{-Z_{\text{ion}}}{r_{\text{loc}}}\sqrt{\frac{2}{\pi}}, \tag{98}$$

and the local pseudopotential is defined at the origin (nucleus), too.

The nonlocal pseudopotential is defined by

$$V_{\text{nonlocal}}[\phi] = \mathbf{r} \in \mathbb{R}^3 \mapsto \sum_l \int V_l(\mathbf{r},\mathbf{r}')\phi(\mathbf{r}')d^3\mathbf{r}', \tag{99}$$

where

$$V_l(\mathbf{r},\mathbf{r}') = \sum_{i=1}^{3}\sum_{j=1}^{3}\sum_{m=-l}^{l} Y_{l,m}(\hat{\mathbf{r}})p_i^l(r)h_{i,j}^l p_j^l(r')Y_{l,m}^*(\hat{\mathbf{r}}') \tag{100}$$

TABLE I. Computation grids. We define $Z(n) := \{k \in \mathbb{Z} : |k| \leqslant n\}$.

Number	Grid points
1	$\frac{1}{2}(Z(20))^3$
2	$\frac{1}{2}(Z(20))^3 \cup \frac{1}{4}(Z(10))^3$
3	$\frac{1}{2}(Z(20))^3 \cup \frac{1}{4}(Z(10))^3 \cup \frac{1}{8}(Z(4) \times Z(4) \times Z(10))$
4	$\frac{1}{4}(Z(60))^3$
5	$\frac{1}{2}(Z(30))^3 \cup \frac{1}{4}(Z(15))^3$
6	$(Z(38))^3 \cup \frac{1}{2}(Z(19))^3$
7	$\frac{1}{4}(Z(40))^3$
8	$(Z(10))^3 \cup \frac{1}{2}(Z(10))^3$
9	$\frac{1}{2}(Z(20))^3 \cup \frac{1}{4}(Z(20))^3$
10	$\frac{1}{4}(Z(40))^3 \cup \frac{1}{8}(Z(40))^3$
11	$(Z(10))^3 \cup \frac{1}{2}(Z(5))^3$
12	$\frac{1}{2}(Z(20))^3 \cup \frac{1}{4}(Z(10))^3 \cup \frac{1}{8}(Z(4) \times Z(4) \times Z(15))$
13	$\frac{1}{4}(Z(40))^3 \cup \frac{1}{8}(Z(20))^3$
14	$\frac{1}{4}(Z(60))^3 \cup \frac{1}{8}(Z(30))^3$

for each nucleus. The origin of the coordinate system in (100) is located at the nucleus. The functions p_i^l are defined by

$$p_i^l(r) = \frac{\sqrt{2} r^{l+2(i-1)} \exp\left(-\frac{r^2}{2r_l^2}\right)}{r_l^{l+(4i-1)/2} \sqrt{\Gamma\left(l + \frac{4i-1}{2}\right)}}, \tag{101}$$

where parameter r_l is given in Bohrs. The range of values l is determined by the actual pseudopotential. The spherical harmonics $Y_{l,m}$ in Eq. (100) can be replaced by orthonormal linear combinations of $Y_{l,m}$, $m = -l, \ldots, l$. This allows us to avoid computation with complex valued functions.

VI. ATOMIC AND MOLECULAR ORBITALS

The hydrogen atom, hydrogen molecule ion, and lithium HGH computations presented here have been performed with the Arnoldi method. The helium, hydrogen molecule, and lithium hydride computations have been performedwith self-consistent iteration and the Arnoldi method. When there is only one resolution level in the basis the Hamiltonian and Laplacian matrices are Hermitian and the Arnoldi method reduces to a variant of the Lanczos method. Furthermore, the ordinary conjugate gradient method could be used for the Poisson equation. Two methods have been used for solving the Poisson equation for the general case: CGNR and GMRES. We ran a benchmark for these methods and GMRES was eight times faster when the accuracies of the results were approximately the same. This is because the GMRES code is parallelized better than CGNR. All the computations use eigth order Deslauriers-Dubuc wavelets (polynomial span 7). We use interpolating polynomials of degree 7 for the pseudopotentials. In some computations, the Arnoldi method did not find the desired eigenvalues. This was solved by rising the number of computed eigenvalues and the number of basis vectors in the Arnoldi method. The basis function sets (computation point grids) are presented in Table I. The grid spacing for a wavelet basis is defined to be $g = 2^{-j_{\max}} a$ where $j_{\max}$ is the maximum resolution level in the basis and a is the size of one unit in resolution level 0 in the wavelet basis in atomic units. See Sec. II A.

TABLE II. Total energy of the hydrogen atom. Quantity g is the distance between grid points in the highest resolution level. The numbers in column 'Basis" refer to Table I and "TH" means this paper.

Source	Basis	g (B)	Pseudopot.	E (Ha)
TH	7	0.25	Const.	−0.487470
TH	8	0.5	Const.	−0.462247
TH	9	0.25	Const.	−0.487470
TH	10	0.125	Const.	−0.496380
TH	7	0.25	Interp.	−0.478328
TH	8	0.5	Interp.	−0.439146
TH	9	0.25	Interp.	−0.478328
TH	10	0.125	Interp.	−0.493471
TH	7	0.25	HGH	−0.499294
TH	8	0.5	HGH	−0.589957
TH	9	0.25	HGH	−0.499295
TH	10	0.125	HGH	−0.499899
CCCBDB [43]				−0.466582
BIGDFT [33,34]			HGH	−0.499969
Exact			None	−0.5

The data presented in the tables in this article were obtained from our own software (denoted by TH), our own computations with BIGDFT [33,34], and CCCBDB [43]. BIGDFT is a quantum-mechanical computation package using Daubechies wavelets. CCCBDB is large database containing atomic and molecular data. The CCCBDB energies and internuclear distances in this article use the (slater-type orbital) STO-3G basis set. Quantity g is the distance between grid points in the highest resolution level, and quantity d is the distance between the nuclei in the result tables. E_{system} is the total energy of the system, and E_{binding} is the binding energy. We used grid spacing 0.45 B (finer grid spacing 0.225 B) in all our BIGDFT computations. The BIGDFT parameters for determining the size of the basis set were crmult=10.0 and frmult=16.0. Parameter crmult is used to specify the size of the coarse region and parameter frmult the size of the fine region around atoms. The

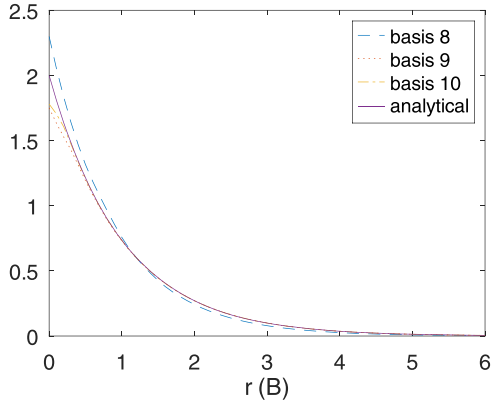

FIG. 2. Radially averaged wave functions of the hydrogen atom for several bases. The solid line is the analytical radial wave function. The basis numbers refer to Table I.

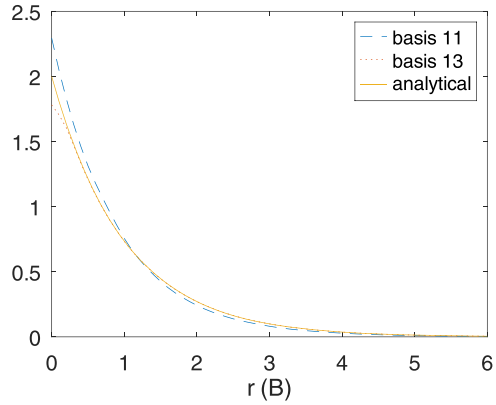

FIG. 3. Radially averaged wave functions of the hydrogen atom for some bases. The solid line is the analytical radial wave function. The basis numbers refer to Table I.

computations were also performed with values crmult = 5.0 and frmult = 8.0, but the results did not differ significantly. Note that the total energy does not include the energies of the core electrons in the lithium hydride HGH computations. Computations using our own software use interpolating wavelets and BIGDFT computations orthonormal Daubechies wavelets.

For the molecular computations, the energy of the system as a function of the distance between the nuclei is computed in three points near the energy minimum, and a second degree polynomial is fitted into these points. The distance between the nuclei is then the minimum point of the polymial, and the energy of the system is computed at the minimum distance. We locate the nuclei at points $(0, 0, \pm\frac{d}{2a})$ where d is the distance between the nuclei in Bohrs. When binding energies of molecules were computed the energies of atoms were usually computed with the basis set as the molecule. When the basis was unsymmetric, it was modified. For example, grid $Z(4)\times Z(4)\times Z(10)$ becomes $Z(4)\times Z(4)\times Z(4)$ for the atoms. See the caption of Table I for the definition of $Z(n)$.

The results for hydrogen atom ground state are presented in Table II. The radially averaged ground state wave functions

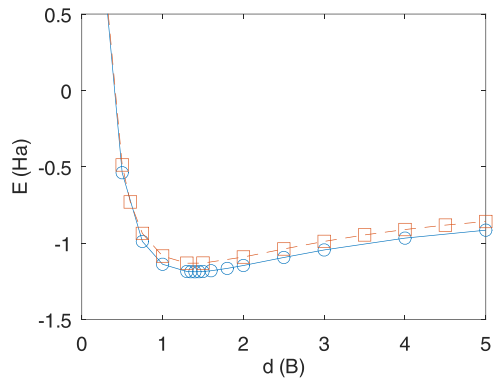

FIG. 4. Energy of H_2 as a function of internuclear distance calculated with the Hartree-Fock method and HGH pseudopotential. The solid line is our computation with interpolating wavelets and basis set 5, $g = 0.25$ B, and the dashed line is computed with BIGDFT and (fine) grid spacing $g = 0.225$ B.

TABLE III. Hydrogen atom orbital energies with the HGH pseudopotential. We labeled the resulting $2p$ orbitals with a, b, and c. All the orbitals presented are approximately orthogonal.

Orbital	Computed energy (Ha)	Exact energy (Ha)
$1s$	−0.499295	−0.5
$2s$	−0.120957	−0.125
$2p_a$	−0.123045	−0.125
$2p_b$	−0.123045	−0.125
$2p_c$	−0.123045	−0.125

of the hydrogen atom are plotted in Figs. 2 and 3. A radial average of a function $f\colon \mathbb{R}^3 \to \mathbb{R}$ is computed by

$$\bar{f}(r) := \frac{1}{4\pi}\int_{\theta=0}^{\pi}\int_{\phi=0}^{2\pi} f(r,\theta,\phi)\sin\theta\, d\phi\, d\theta, \qquad (102)$$

where $r \in [0, \infty[$. As the angular part of a s-type wave function is $\frac{1}{2\sqrt{\pi}}$, we estimate a radial wave function by

$$\bar{g}(r) := \frac{1}{2\sqrt{\pi}}\int_{\theta=0}^{\pi}\int_{\phi=0}^{2\pi} f(r,\theta,\phi)\sin\theta\, d\phi\, d\theta. \qquad (103)$$

The calculation of hydrogen excited states uses HGH pseudopotential and basis 9. Results are presented in Table III. The names of the excited states were obtained by computing inner products between the computed states and analytical states. The resulting orbitals are approximately orthonormal and the computed $2p$ states are approximately linear combinations of the analytical $2p$ states. The largest (in absolute value) inner product between different orbitals is $\langle 2p_a|2p_c\rangle = 5.428\times10^{-4}$. The quality of the linear combinations can be measured by a quantity $\sqrt{1-\|Pf\|_2^2}$ where P is the orthogonal projection from $L^2(\mathbb{R}^3)$ onto the space spanned by $2p_x$, $2p_y$, and $2p_z$. The value of this quantity is 0.1265 for all the computed orbitals $2p_a$, $2p_b$, and $2p_c$. Analytical expressions for hydrogenic orbitals can be found for example in Ref. [46].

Helium atom has been computed using the HGH pseudopotential. Results are presented in Table IV. Grid spacing $g = 0.5$ B does not give sensible results with the HGH pseudopotential. We suppose that Froese Fischer's results [44]

TABLE IV. Energetics of the helium atom. All our and BIGDFT computations use the HGH pseudopotential. The numbers in column Basis refer to Table I and TH means this paper.

Source	Basis	g (B)	Exchange potential	E (Ha)	E_{orb} (Ha)
TH	4	0.25	HF	−2.901959	−0.971927
TH	5	0.25	HF	−2.901180	−0.970247
TH	4	0.25	LDA	−2.821511	−0.629713
TH	5	0.25	LDA	−2.819951	−0.628152
TH	14	0.125	HF	−2.916129	−0.974768
CCCBDB [43]			HF	−2.807584	
CCCBDB [43]			LSDA	−2.809599	
BIGDFT [33,34]			HF	−2.862303	
BIGDFT [33,34]			LDA	−2.833895	
HF limit [44]			HF	−2.862	−0.918

TABLE V. Hydrogen molecule. The numbers in columnBasis refer to Table I and TH means this paper.

Source	Basis	a (B)	g (B)	Pseudopot.	Exch.	E_{system} (Ha)	E_{binding} (Ha)	d (B)
TH	1	1.0	0.5	interp.	HF	−1.045883	0.167601	1.855140
TH	2	1.0	0.25	interp.	HF	−1.156554	0.199450	1.501870
TH	3	1.0	0.125	interp.	HF	−1.186176	0.210390	1.454593
TH	4	1.0	0.25	HGH	HF	−1.188779	0.190189	1.397995
TH	5	1.0	0.25	HGH	HF	−1.187995	0.189405	1.397991
TH	6	0.4	0.20	HGH	HF	−1.188547	0.189383	1.389890
TH	4	1.0	0.25	HGH	LDA	−1.157528	0.158938	1.485861
TH	5	1.0	0.25	HGH	LDA	−1.155960	0.157378	1.485851
CCCBDB[a]					HF	−1.117506	0.184342	1.345
CCCBDB[a]					LSDA	−1.157014	0.248654	1.391
BIGDFT[b]				HGH	HF	−1.133393	0.133455	1.386175
BIGDFT[b]				HGH	LDA	−1.136870	0.136932	1.445097
Experimental[c]							0.166	1.40

[a]Reference [43].
[b]Reference [33,34].
[c]Reference [45], Chap. 5.2.

can be regarded as the Hartree-Fock limit for helium. The computed total energies of the helium atom are quite good.

We calculated the hydrogen molecule with the interpolated and HGH pseudopotentials. The computation results for the hydrogen molecule are presented in Table V. The resulting dissociation curve with the HF method, HGH pseudopotential, and basis set 5 is plotted in Fig. 4. When the HGH pseudopotential was used the computation worked for grid spacing $g = 0.25$ B but did not work for spacing $g = 0.5$ B. The minimum energy of the curve is $E_0 = -1.188$ Ha, and it is located at internuclear distance $d_0 = 1.398$ B. The corresponding values for the BIGDFT reference curve are $E_0 = -1.132$ Ha and $d_0 = 1.385$ B. The results for the hydrogen molecule ion are presented in Table VI.

The calculations for lithium hydride molecule are presented in Table VII. Grid spacing $g = 0.5$ B did not yield a physical dissociation curve for the HGH pseudopotential. Neither $g = 0.5$ B nor $g = 0.25$ B yielded a physical dissociation curve for the interpolated pseudopotential. The dissociation curve of lithium hydride computed with the Hartree-Fock method and basis set 5 is plotted in Fig. 5. The minimum energy of the curve is $E_0 = -0.817$ Ha, and it is located at internuclear distance $d_0 = 2.880$ B. The corresponding values for the BIGDFT reference curve are $E_0 = -0.760$ Ha and $d_0 = 2.921$ B.

The energies of the hydrogen atom converge to the exact value for the constant, interpolated, and HGH pseudopotentials with grid spacings $g = 0.5$, 0.25, and 0.125 B (Table II). The Hartree-Fock helium computations yield approximately same results for $g = 0.25$ B and $g = 0.125$ B (Table IV). The Hartree-Fock computations of the hydrogen molecule using the HGH pseudopotential give approximately same energies for $g = 0.25$ B and $g = 0.2$ B (Table V). The calculations of the hydrogen molecule ion using the HGH pseudopotential yield approximately same energies and internuclear distances for $g = 0.25$ B and $g = 0.125$ B (Table VI). The Hartree-Fock computations of the lithium hydride molecule give approximately same results for $g = 0.25$ B and $g = 0.2$ B (Table VII).

TABLE VI. Hydrogen molecule ion H_2^+. The analytical results are equal to the experimental results. The numbers in column Basis refer to Table I and TH means this paper.

Source	Basis	g (B)	Pseudopot.	E_{system} (Ha)	E_{binding} (Ha)	d (B)
TH	1	0.5	interp.	−0.520169	0.082028	2.371005
TH	2	0.25	interp.	−0.573665	0.095310	2.021654
TH	12	0.125	interp.	−0.589135	0.101242	2.015143
TH	11	0.5	HGH	−0.712279	0.121898	2.007951
TH	2	0.25	HGH	−0.601783	0.102460	2.006845
TH	7	0.25	HGH	−0.601636	0.102342	2.005329
TH	13	0.125	HGH	−0.602448	0.102549	1.999338
CCCBDB[a]				−0.582697	0.116115	2.005
BigDFT[b]			HGH	−0.602489	0.102520	1.995677
Experimental[c]					0.103	2.00

[a]Reference [43].
[b]Reference [33,34].
[c]Reference [45], Chap. 4.6.

TABLE VII. Lithium hydride molecule. All our and BIGDFT computations were performed with the HGH pseudopotential. The CCCBDB all-electron total energies are not presented in the table because the energies calculated by us do not include the energies of the core electrons. The numbers in column Basis refer to Table I and TH means this paper.

Source	Basis	a (B)	g (B)	Exch.	E_{system} (Ha)	E_{binding} (Ha)	d (B)
TH	4	1.0	0.25	HF	−0.817817	0.117472	2.879961
TH	5	1.0	0.25	HF	−0.817030	0.116686	2.880018
TH	4	1.0	0.25	LDA	−0.811482	0.111137	3.013411
TH	5	1.0	0.25	LDA	−0.809904	0.109560	3.013474
TH	6	0.4	0.2	HF	−0.817007	0.116370	2.863496
CCCBDB[a]				HF		0.081274	2.855
CCCBDB[b]				LSDA		0.135698	2.899
BIGDFT[b]				HF	−0.760938	0.059911	2.866004
BIGDFT[b]				LDA	−0.776416	0.075389	2.930745

[a]Reference [43].
[b]References [33,34].

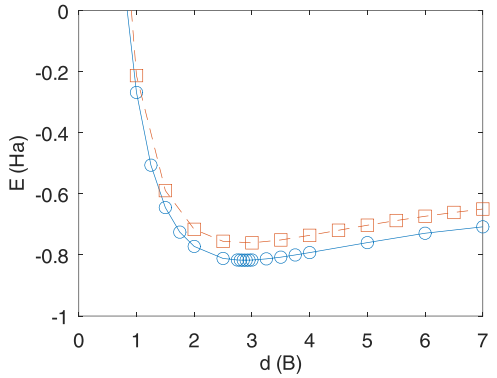

FIG. 5. Total energy of the lithium hydride molecule as a function of the internuclear distance calculated with the Hartree-Fock method and HGH pseudopotential. The solid line has been computed with interpolating wavelets and basis set 5, $g = 0.25$ B, and the dashed line with BIGDFT and (fine) grid spacing $g = 0.225$ B.

VII. CONCLUSIONS

We have shown how to solve the wave equations of hydrogen and helium atoms, hydrogen molecule ion, and hydrogen and lithium hydride molecules in a three-dimensional interpolating tensor product wavelet basis. As far the authors know, only Arias [10] and Engeness and Arias [11] have performed this before. However, they do not use the dual interpolating MRA to evaluate matrix elements. We do that, and it allows us to neglect the overlap integrals of the basis functions.

It seems to require large basis sets to obtain numerically good orbitals for quantum physical systems. Roughly, the description requires, at least, 10 000 basis functions. The most accurate computed bond length of the hydrogen molecule is good and the energy satisfactory. The most accurate binding energies and internuclear distances for the hydrogen molecule ion in Table VI are very accurate. The calculations with the HGH pseudopotential performed very well with grid spacing $g = 0.25$ B but not with $g = 0.5$ B. The same phenomenon was observed with BIGDFT, too.

We tested the H and He atom computations with BIGDFT so that the coarse grid spacing was changed from 0.45 to 0.225 B. For some reason, we got slightly worse energies. We also found that one level basis set can be replaced with considerably smaller two-level basis set without a significant effect on the results.

Note that having no more than two resolution levels in the basis makes the computation of the Laplacian operator simpler and faster because in that case the $s(\cdots)$ terms in the Laplacian operator, equations (60)–(62), are either Kronecker δs or zero.

[1] I. Daubechies, *Ten Lectures on Wavelets*, CBMS-NSF Regional Conference Series in Applied Mathematics 61 (SIAM, Philadelphia, 1992).
[2] C. K. Chui and C. Li, SIAM J. Math. Anal. **27**, 865 (1996).
[3] D. L. Donoho, Interpolating Wavelet Transforms, Technical Report No. 408 (Department of Statistics, Stanford University, Stanford, 1992).
[4] G. Deslauriers and S. Dubuc, Constr. Approx. **5**, 49 (1989).
[5] S. Dubuc, J. Math. Anal. Appl. **114**, 185 (1986).
[6] T. Höynälänmaa, Int. J. Wavelets Multiresolut Inf. Process. **13**, 1550010 (2015).
[7] S. Goedecker, *Wavelets and Their Application for the Solution of Partial Differential Equations in Physics* (EPFL Press, Lausanne, 1998).
[8] N. Fukuda, T. Kinoshita, and T. Suzuki, Int. J. Wavelets Multiresolut Inf. Process. **14**, 1650007 (2016).
[9] R. S. Pathak, Int. J. Wavelets Multiresolut Inf. Process. **9**, 905 (2011).
[10] T. A. Arias, Rev. Mod. Phys. **71**, 267 (1999).
[11] T. D. Engeness and T. A. Arias, Phys. Rev. B **65**, 165106 (2002).
[12] R. A. Lippert, T. A. Arias, and A. Edelman, J. Comput. Phys. **140**, 278 (1998).
[13] P. Fischer and M. Defranceschi, SIAM J. Numer. Anal. **35**, 1 (1998).
[14] P. Fischer and M. Defranceschi, *Wavelet Analysis and Its Applications*, Vol. 5 (Academic Press, 1994),pp. 495–506.
[15] P. Fischer and M. Defranceschi, Appl. Comput. Harmon. Anal. **1**, 232 (1994).
[16] S. Wei and M. Y. Chou, Phys. Rev. Lett. **76**, 2650 (1996).
[17] C. J. Tymczak and X.-Q. Wang, Phys. Rev. Lett. **78**, 3654 (1997).
[18] K. Yamaguchi and T. Mukoyama, Nucl. Instrum. Methods Phys. Res. Sect. B **124**, 361 (1997).
[19] T. Höynälänmaa, T. T. Rantala, and K. Ruotsalainen, Phys. Rev. E **70**, 066701 (2004).
[20] T. Höynälänmaa and T. T. Rantala, Atoms **11**, 9 (2023).
[21] S. S. Iyengar and M. J. Frisch, J. Chem. Phys. **121**, 5061 (2004).
[22] C. J. Tymczak, A. M. N. Niklasson, and H. Röder, J. Comput. Phys. **175**, 363 (2002).
[23] G. Strang and V. Strela, Opt. Eng. **33**, 2104 (1994).
[24] F. Gossler, B. Oliveira, M. Duarte, J. Vieira Filho, F. Villarreal, and R. Lamblém, Trends Comput. Appl. Math. **22**, 139 (2021).
[25] A. Singh and J. Singh, Indian J. Sci. Technol. **9**, 1 (2016).
[26] R. J. Harrison, G. I. Fann, T. Yanai, and G. Beylkin, in *Computational Science–ICCS 2003: International Conference, Melbourne, Australia and St. Petersburg, Russia, June 2–4, 2003 Proceedings, Part IV 3* (Springer, Berlin, Heidelberg, 2003), pp. 103–110.
[27] T. Yanai, G. I. Fann, Z. Gan, R. J. Harrison, and G. Beylkin, J. Chem. Phys. **121**, 6680 (2004).
[28] T. Yanai, R. J. Harrison, and N. C. Handy, Mol. Phys. **103**, 413 (2005).
[29] T. Yanai, G. I. Fann, G. Beylkin, and R. J. Harrison, Phys. Chem. Chem. Phys. **17**, 31405 (2015).
[30] S. R. Jensen, S. Saha, J. A. Flores-Livas, W. Huhn, V. Blum, S. Goedecker, and L. Frediani, J. Phys. Chem. Lett. **8**, 1449 (2017).
[31] S. R. Jensen, T. Flå, D. Jonsson, R. S. Monstad, K. Ruud, and L. Frediani, Phys. Chem. Chem. Phys. **18**, 21145 (2016).
[32] S. Han, K. Cho, and J. Ihm, Phys. Rev. B **60**, 1437 (1999).
[33] L. Genovese *et al.*, J. Chem. Phys. **129**, 014109 (2008).
[34] S. Mohr *et al.*, J. Chem. Phys. **140**, 204110 (2014).

[35] W. E. Arnoldi, Q. Appl. Math. **9**, 17 (1951).
[36] R. B. Lehoucq and D. C. Sorensen, SIAM J. Matrix Anal. Appl. **17**, 789 (1996).
[37] Y. Saad, J. R. Chelikowsky, and S. M. Shontz, SIAM Rev. **52**, 3 (2010).
[38] Y. Saad and M. H. Schultz, SIAM J. Sci. Statist. Comput. **7**, 856 (1986).
[39] W. Kohn, Rev. Mod. Phys. **71**, 1253 (1999).
[40] J. M. Soler, E. Artacho, J. D. Gale, A. García, J. Junquera, P. Ordejón, and D. Sánchez-Portal, J. Phys.: Condens. Matter **14**, 2745 (2002).
[41] O. V. Vasilyev and P. Paolucci, J. Comput. Phys. **125**, 498 (1996).
[42] C. Hartwigsen, S. Goedecker, and J. Hutter, Phys. Rev. B **58**, 3641 (1998).
[43] http://cccbdb.nist.gov
[44] C. Froese Fischer, *The Hartree–Fock Method for Atoms–A Numerical Approach* (Wiley, New York, 1977).
[45] L. van Dommelen, Quantum Mechanics for Engineers, http://www.umich.edu/~ners312/CourseLibrary/Dommelen.pdf
[46] P. Atkins and R. Friedman, *Molecular Quantum Mechanics* (Oxford University Press, New York, 2005).